JOURNAL OF MATERIALS SCIENCE 28 (1993) 1525–1531

Ar^+-ion sputtering-induced surface topography development on aluminium

A. K. SEN, D. GHOSE
Saha Institute of Nuclear Physics, Sector-1, Block-"AF", Bidhan Nagar, Calcutta 700 064, India

The surface topography of aluminium after bombardment with a mass-separated obliquely incident Ar^+ beam while simultaneously supplying gold or tungsten "seeds", as well as under unseeded conditions, was studied by scanning electron microscopy. The sputtered topography was characterized mainly by cones. It was noted that seeding did not necessarily always enhance the cone population, as is widely believed. The expression for the cone apex angle derived from the first-order erosion theory for normal cones was found to predict equally well that for oblique cones. The formation of tailed cones, coalescence of closely packed cones, bending of cones and disintegration of the cone apex were observed and are discussed. Finally, the corrugated terraced morphology developed on some grains was similar in nature to that observed on semiconductors rendered amorphous under ion bombardment.

1. Introduction

Solid surfaces subjected to energetic ion bombardment generally develop characteristic surface structures due to sputtering. Cones, pyramids, pits, hillocks, steps, etc., have been observed. Most of the gross features of ion bombardment-induced surface topography can be described well by the first-order erosion theory [1], which is based mainly on the dependence of the sputtering yield on the angle of ion-beam incidence to the surface normal. However, other detailed features are rather difficult to understand without so-called secondary effects such as ion reflection, redeposition of sputtered particles and surface diffusion of atoms. Textured surfaces formed by ion-beam sputtering offer an opportunity for a fundamental understanding of the ion–solid interaction processes, and such surfaces are also interesting in a technological perspective [2].

The most frequently appearing sputtering structures on ion-bombarded metal surfaces are cones or pyramids. They can form due to the presence of impurities or asperities on the surface or due to surface and subsurface defects and dislocations induced by the ion–atom collisions [3]. A full understanding of the physical processes involved has not yet been established.

Most of the investigations on cone formation were carried out on copper targets and also with normally incident ions. Studies on other metals and the effects resulting from non-normal ion-beam incidence are relatively rare. The present work is concerned with the topographical modifications of aluminium surfaces by energetic Ar^+-ion bombardment. Both impurity seeded and pure, initially smooth, surfaces have been bombarded. Because aluminium is a weakly sputtered material [4], the bombardment was performed at oblique incidence to enhance erosion, so that the sputtering-induced structures would be well developed.

2. Experimental procedure

The experiment was carried out in an electromagnetic isotope separator of Bernas type [5], which provides an intense and isotopically pure ion beam. Aluminium polycrystals (99.9% pure), 24 mm diameter and 6 mm thick, were used as targets. The surfaces were mechanically polished first with a dry 600 grit paper and finally with 1 μm alumina powder with water in the Minimet polisher (Buehler Ltd, USA), followed by cleaning in alcohol in an Ultramet sonic cleaner (Buehler Ltd, USA). The sputtering was done by 30 keV $^{40}Ar^+$ ions incident on the target at an angle of approximately 58° to the surface normal. In some bombardments, high-melting impurities such as gold or tungsten were simultaneously seeded (flux $\sim 10^{16}$ particles $cm^{-2}s^{-1}$), because they are known to promote cone formation [6]. The seed material was in the form of a thin foil or wire and was placed in the centre of the ion-beam cross-section at the surface. To minimize the contamination of the target surface by foreign atoms coming from the beam-defining aperture, the latter was made of the same aluminium material. The ion current density was > 100 μA cm^{-2} and the residual gas pressure was around 10^{-5} torr (1 torr = 133.322 Pa). The ion dose ranged from $9 \times 10^{18} - 5 \times 10^{19}$ ions cm^{-2} measured by a Danfysik 554 current integrator after suppression of the ion-induced secondary electron emission. The irradiated surfaces were examined in a Philips PSEM 500 scanning electron microscope (SEM).

3. Results and discussion

An electron micrograph of the unbombarded surface is shown in Fig. 1 where it is clear that the surface is flat and smooth except for some fine scratch marks and dust particles left on the surface. Fig. 2 shows an electron micrograph of the sputtered surface. The

0022–2461

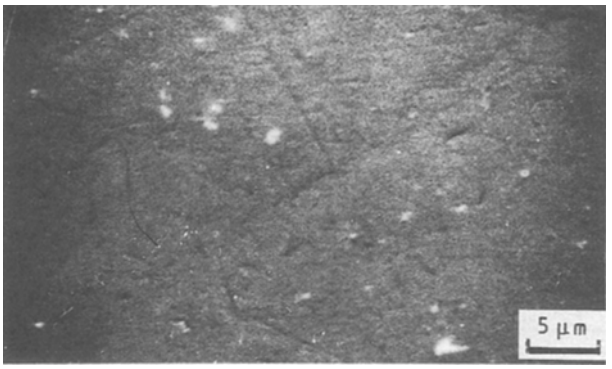

Figure 1 Electron micrograph of the polished aluminium surface.

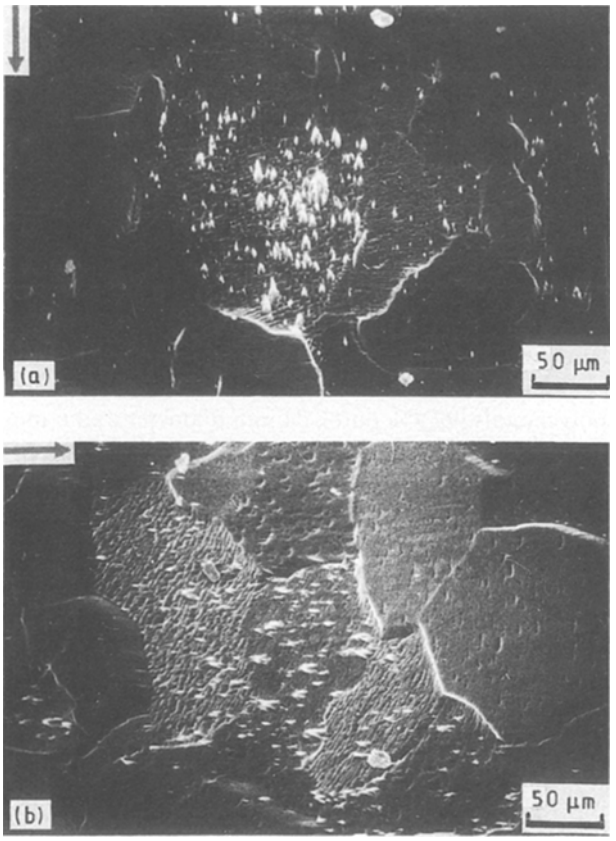

Figure 2 Electron micrographs of an unseeded aluminium surface at two different regions after bombardment with a dose of 9×10^{18} ions cm^{-2}. The white dots are revealed to be the expected cones when observed at higher magnification. The arrow indicates the direction of ion incidence.

general observations are the delineation of individual crystal grains with single slopes formed at the grain boundaries, and the development of structures on some grains. The grain size varies from 85–230 μm. Similar topographical features are also obtained on gold- or tungsten-seeded surfaces.

For crystalline metals, the sputtering yield varies with orientation with sharp minima in the low-index directions due to channelling of the incident ions. The effect of this on polycrystalline specimens is that grains of different orientation will etch at different rates. At high enough doses the difference in yield results in a step forming between the grains. Fig. 2 also reveals that the morphological structures of individual grains are quite different. A number of grains develop conical protrusions, etch pits, corrugations and terraces, while the others are simply eroded with no characteristic etch patterns at all.

Cone formation in metal targets has been the subject of extensive studies, as is evident in recent literature [3]. Fig. 3 shows an eroded grain of gold-seeded surface containing sharp cones. For impurity-induced cone development, low sputtering yield materials were believed to be essential until recently, when Wehner [6] experimentally found that seed metal should be of a higher melting point than the substrate and that the relative sputtering yield is unimportant. In the mechanism of cone formation under continuous seed supply, the presence of seed clusters is a prerequisite for cone nucleation [7, 8]. The seed clustering arises from the surface diffusion of seed atoms, and there is a critical temperature, T_c, to trigger the surface diffusion required for sustaining clusters of minimum size. Assuming the activation energy of seed atoms for surface diffusion in aluminium is ~ 1 eV [8], $T_c \approx 600$ K, which is quite high. However, the necessary surface mobility can also be provided by energetic (> 1 keV) ion impact [6, 8, 9]. In the present experiment, by intentional seeding with high-melting gold or tungsten, no higher probability of cone formation than the unseeded conditions was found. Also, under identical bombardment conditions, not all grains were found to

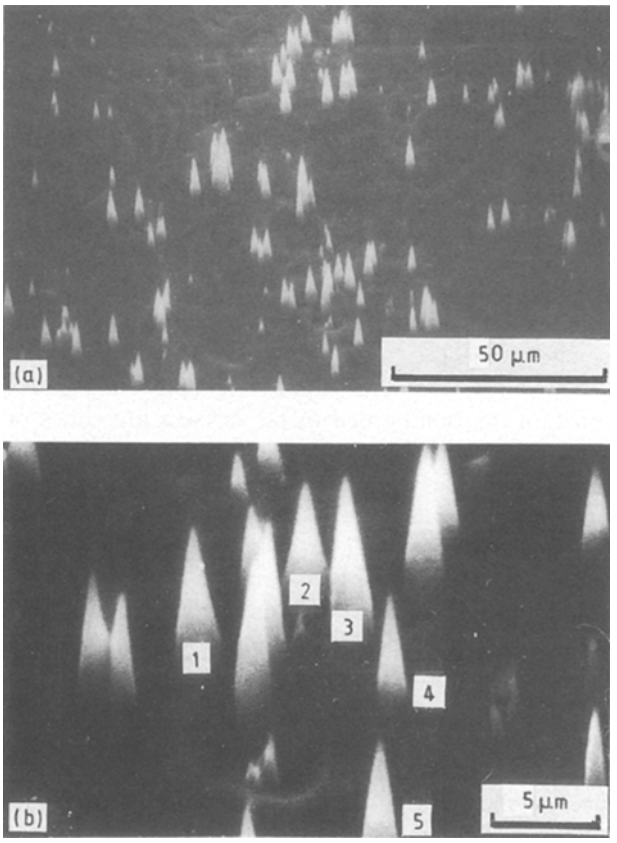

Figure 3 (a) Electron micrograph of the gold-seeded aluminium surface showing a grain containing well-defined cones. (b) A higher magnification micrograph of a region in (a). The apex angles of the cones marked as 1, 2, ... , etc. in (b) are measured; dose = 9×10^{18} ions cm^{-2}.

have cones. These findings are compatible with our previous results on copper [10, 11] and simply indicate that local crystal orientation is the most important parameter for the development of cones. In passing, it should be mentioned that according to Wehner's estimation [6], the critical seed flux for creation of cones is 0.2%, while others [8] estimated it to be $\sim$ 0.1%. Energy dispersive X-ray (EDX) analysis on the irradiated samples with seed material showed that the impurity levels present were of that order. For example, 0.13–0.19 at % Au and 0.4–0.88 at % Ar were detected in different positions of the sputtered gold-seeded surface.

Because the ion beam was incident at some angle to the surface normal, the axes of the cones were tilted away from the surface normal and aligned approximately with the ion beam, as expected from consideration of primary erosion process. Thus the various mechanisms proposed for normal cone formation [3] could, in principle, be applicable for the oblique case, provided that the co-ordinate system is rotated through that angle. The first-order erosion theory relates the cone apex angle, α, to $\hat{\theta}$, the angle for maximum sputtering yield, by the relationship

$$\alpha = 180^\circ - 2\hat{\theta} \tag{1}$$

All calculations that predict cone apex angle are based on the same calculated planar potential from Lindhard [12] :

$$Y(y) = n^{2/3} \int_0^\infty 2\pi r dr\, V(y^2 + r^2)^{1/2} \tag{2}$$

where n is the atomic density of the plane, y the distance of the ion from the plane, and $V(R)$ the ion–atom potential for separation R. Various theoretical predictions of α are available because of different selections of the ion–atom potential [13, 14]. More recently, it was shown that both the Thomas–Fermi–Molière (TFM) potential [15] and the universal potential [16] of Ziegler–Biersack–Littmark (ZBL) are good approximations to the ion–atom interaction potential in low-energy ion scattering [17]. Following the procedure outlined by Witcomb [13], α is calculated using these two potentials [10]

$$\alpha_{\mathrm{TFM}} = 678\left[\frac{n^{2/3}Z_1Z_2}{(Z_1^{1/2} + Z_2^{1/2})^{2/3}E}\right]^{1/2} \tag{3}$$

and

$$\alpha_{\mathrm{ZBL}} = 634\left[\frac{n^{2/3}Z_1Z_2}{(Z_1^{0.23} + Z_2^{0.23})E}\right]^{1/2} \tag{4}$$

TABLE I Comparison of the observed and predicted cone apex angles

Cone number as marked in Fig. 3b	α (exp) (deg)	α (theor) (deg)
1	13.3	11.83
2	14.2	From Eq. 3
3	10.8	11.34
4	13.6	From Eq. 4
5	11.3	

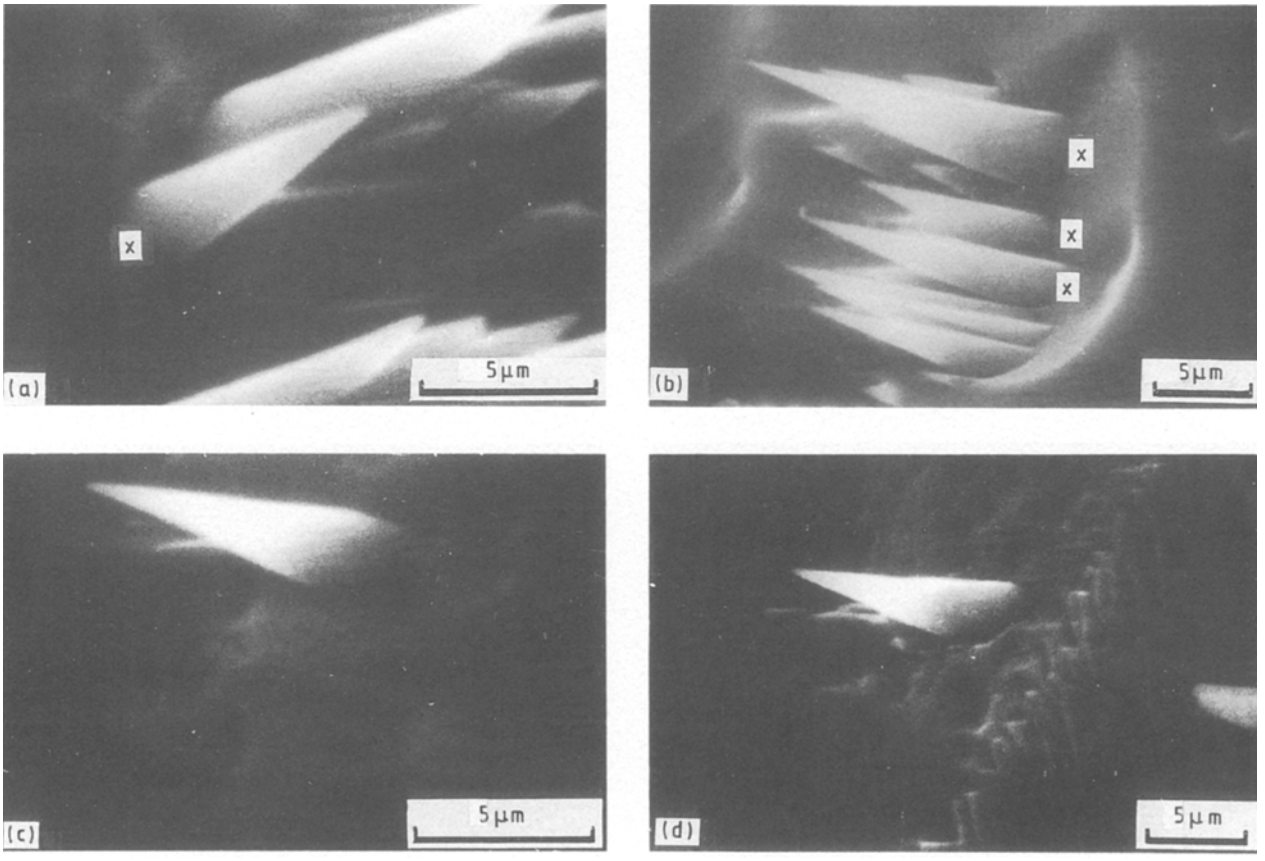

Figure 4 Electron micrographs of the side-view of the cones. The cones marked × have a sloped ridge. In (a) and (b) the surface is seeded with tungsten (c) with gold and (d) unseeded; dose = 5×10^{19} ions/cm^2 in (a) and (b) and 9×10^{18} ions cm^{-2} in (c) and (d).

where Z_1, Z_2 are the ion and target atomic numbers, E the ion energy (eV) and n the number of target atoms (10^3 nm^{-3}). Table I compares the measured α values of some typical cones shown in Fig. 3b, with the calculated ones. The agreement between the theory and experiment is quite satisfactory.

One of the characteristics of oblique cone evolution is the formation of a sloped ridge meeting the cone at the acute-angle side [18–20]. This can be clearly seen from the side view of the cones (Fig. 4). Such an "up-stream" tail is called a "latent plane" by Lewis *et al.* [18] and can be explained by the method of characteristics developed by Carter and Nobes [21].

On some grains a cluster of cones is observed (Fig. 5), especially for the samples which were seeded. In some cases, the cones are so close together that they appear to be fused themselves. The coalescence of closely spaced cones into a so-called "supercone" at high enough doses was recently reported by Nindi and Stulik [22]. It was hypothesized that the valley between the cones became filled up with sputtered material with proceeding ion bombardment, thereby tending to join them together. However, it would not necessarily be expected that all cones develop from one asperity. Two or three agglomerated asperities originating from impurities may be present on the surface. The effect of subsequent sputtering often causes such a structure to transform into a composite of several neighbouring cones which grow together. It is also noted that, in some cases, a single cone has multiple apices (Fig. 6). Morishita and Okuyama [23] investigated a similar phenomenon and suggested that this may happen when the upper cone slopes receive high fluxes of seed atoms. The crystalline seed overlayer that grows epitaxially is believed to cause striations resembling ribbon-like configurations and subsequently a striated cone slope leads to a split in the cone tip.

SEM studies occasionally reveal bent or twisted cones, as illustrated in some selected electron micrographs (Fig. 7; see also Figs 5d and 6b). Belson and Wilson [24] attributed the effect to bending under the stress associated with the surface tension. Because the ratio of surface to volume atomic densities is lower steeply towards the apex, conical projections generally suffer a surface stress that increasingly intensifies as the apex is approached [25]. For certain cone orientations there may be an asymmetry in the resolved shear stresses amongst the slip planes ($\{111\}$ for an f c c lattice). If the surface stress exceeds the critical shear stress, σ_{crit}, the cones seek to minimize their free surface energy by bending or twisting near the tops. A simple analysis leads to the evaluation of the critical shear stress by the equation [24]

$$\sigma_{crit} = \frac{s}{d \tan \alpha/2} \tag{5}$$

where s is the surface tension, $\alpha/2$ the half apex-angle and d the distance from the apex along a generator. From a comparison of two identical cones of which one is slipped as shown in Fig. 5d, the d value is estimated to be 3.8 μm. Assuming $s = 1.03$ N m^{-1} [26], σ_{crit} of aluminium is found to be

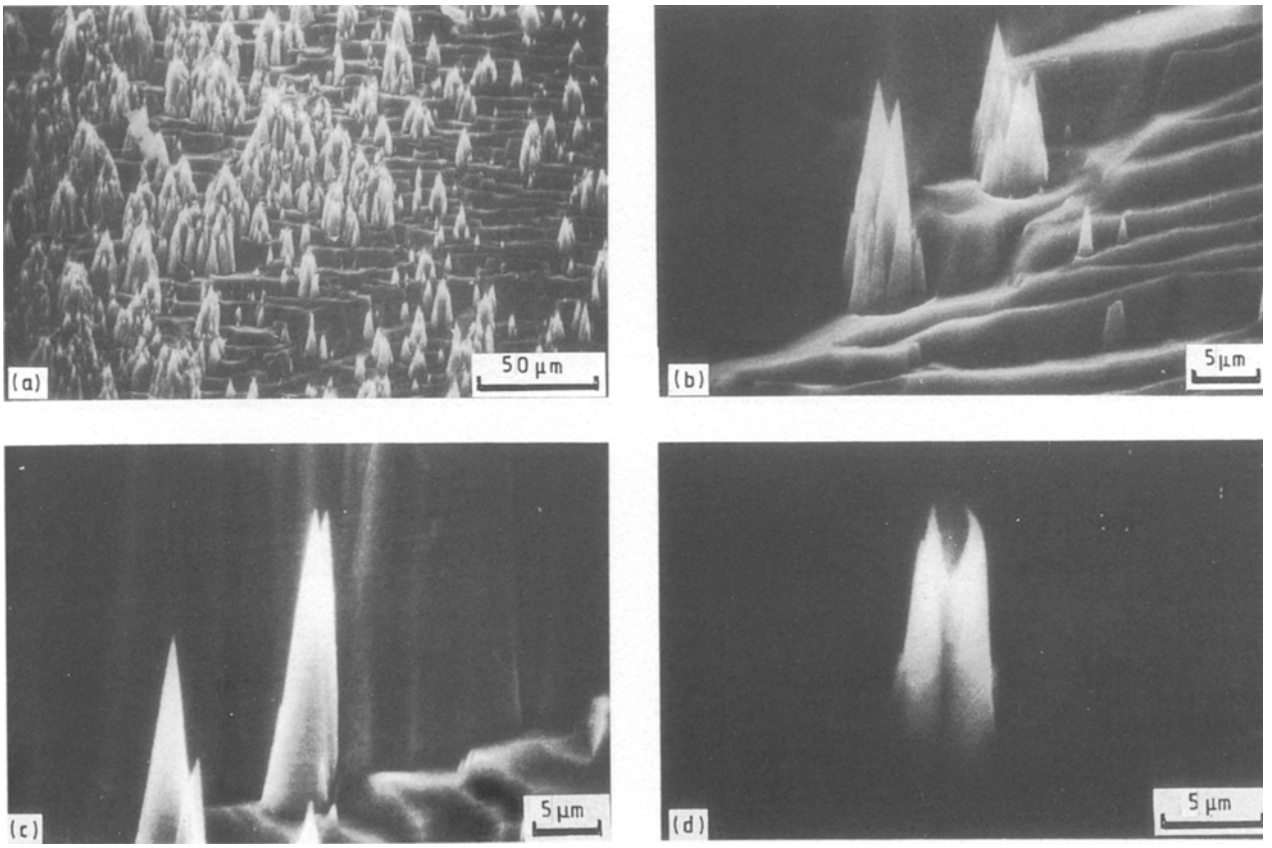

Figure 5 (a) Electron micrograph showing a cluster of cones and fusion of cones on a tungsten-seeded surface. In (b–d) some isolated fused cones are shown at higher magnifications. Note in (d) that the apex of one of the cones is bent; dose = 5×10^{19} ions cm^{-2}.

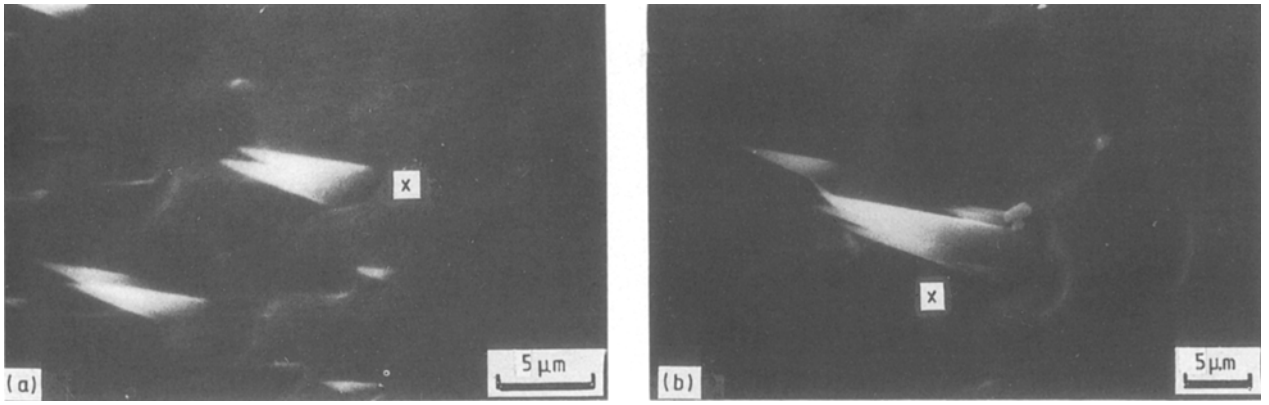

Figure 6 Electron micrographs showing cones marked × with split apex. In (a) the apex is split into two, and in (b) into three parts, of which one is bent. (a) gold-seeded, (b) tungsten-seeded surface; dose = 9×10^{18} ions cm^{-2} in (a) and 5×10^{19} ions cm^{-2} in (b).

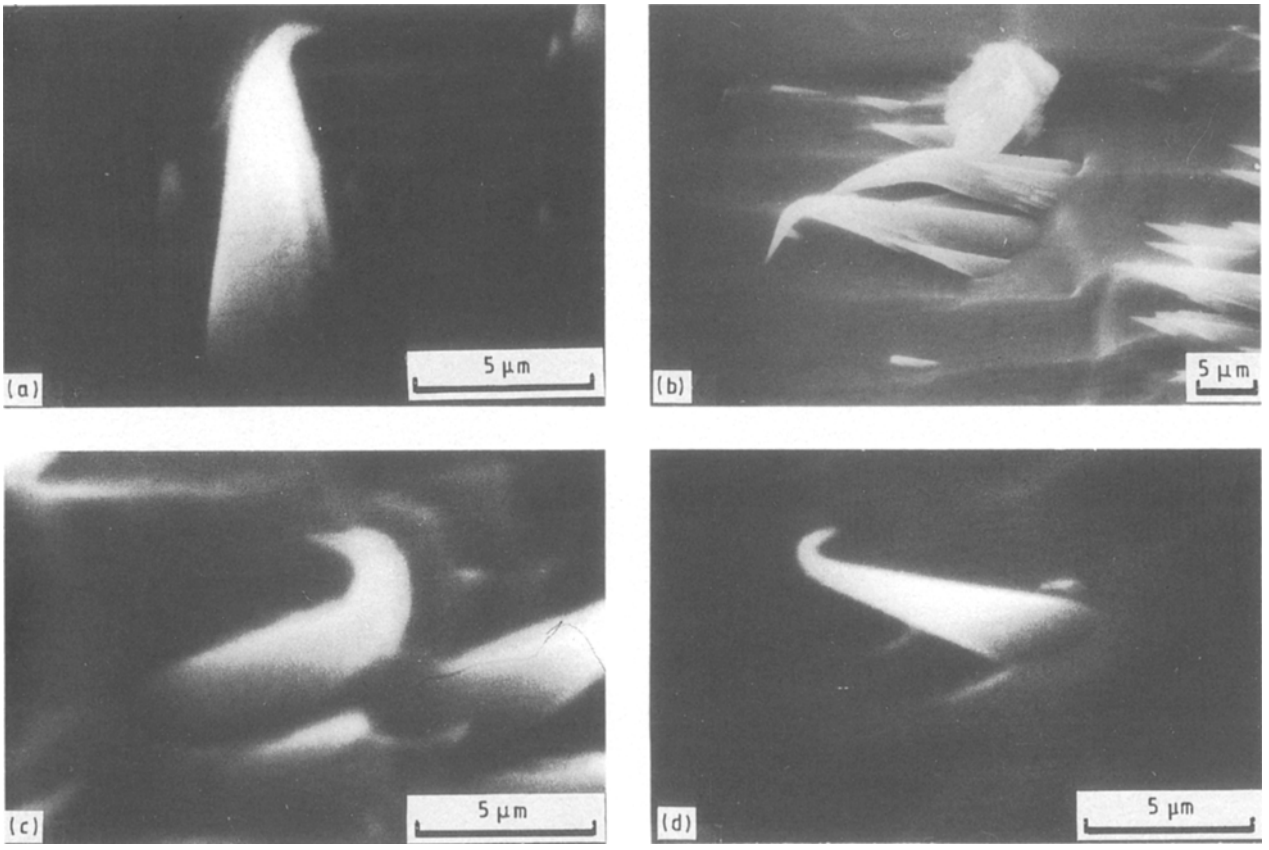

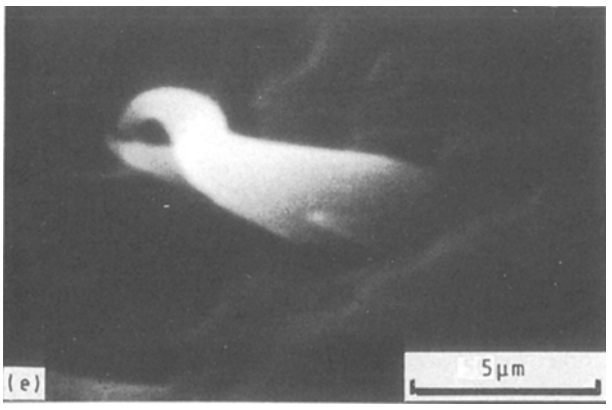

Figure 7 Electron micrographs of deformed cones. In (a) the surface is unseeded, (b, c) seeded with tungsten and (d, e) seeded with gold; dose = 9×10^{18} ions cm^{-2} in (a, d and e) and 5×10^{19} ions cm^{-2} in (b, and c).

2.7×10^6 N m^{-2}. The various morphologies of deformed cones predicted for different inclinations of slip planes [24] are consistent with the present observations. Quite recently, Wehner [6] has pointed out that the bent cones may also be the consequence of the redeposition of atoms sputtered from the neighbouring area. Because the rate of redeposition on the acute-angle side facing the matrix plateau is higher than that on the obtuse-angle side, this causes not only an asymmetry of the surface stresses responsible for bending, but also leads to a slight deviation of the cone axis from the ion-beam direction.

Fig. 8 presents the apex view of the cones. Close inspection reveals that a large number of cones exhibit faceting to varying degrees. Because the average cone base diameter (≈ 3 μm) is far less than the size of the grains, the observed faceting is a single-crystal effect.

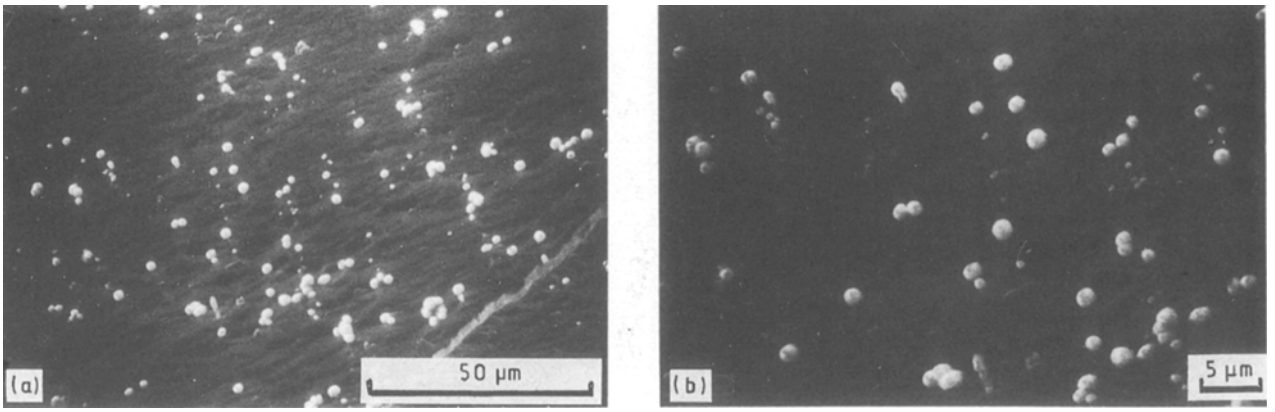

Figure 8 (a) Electron micrograph of the apex view of cones in a gold-seeded aluminium surface. (b) A higher magnification micrograph of (a); dose = 9×10^{18} ions cm^{-2}.

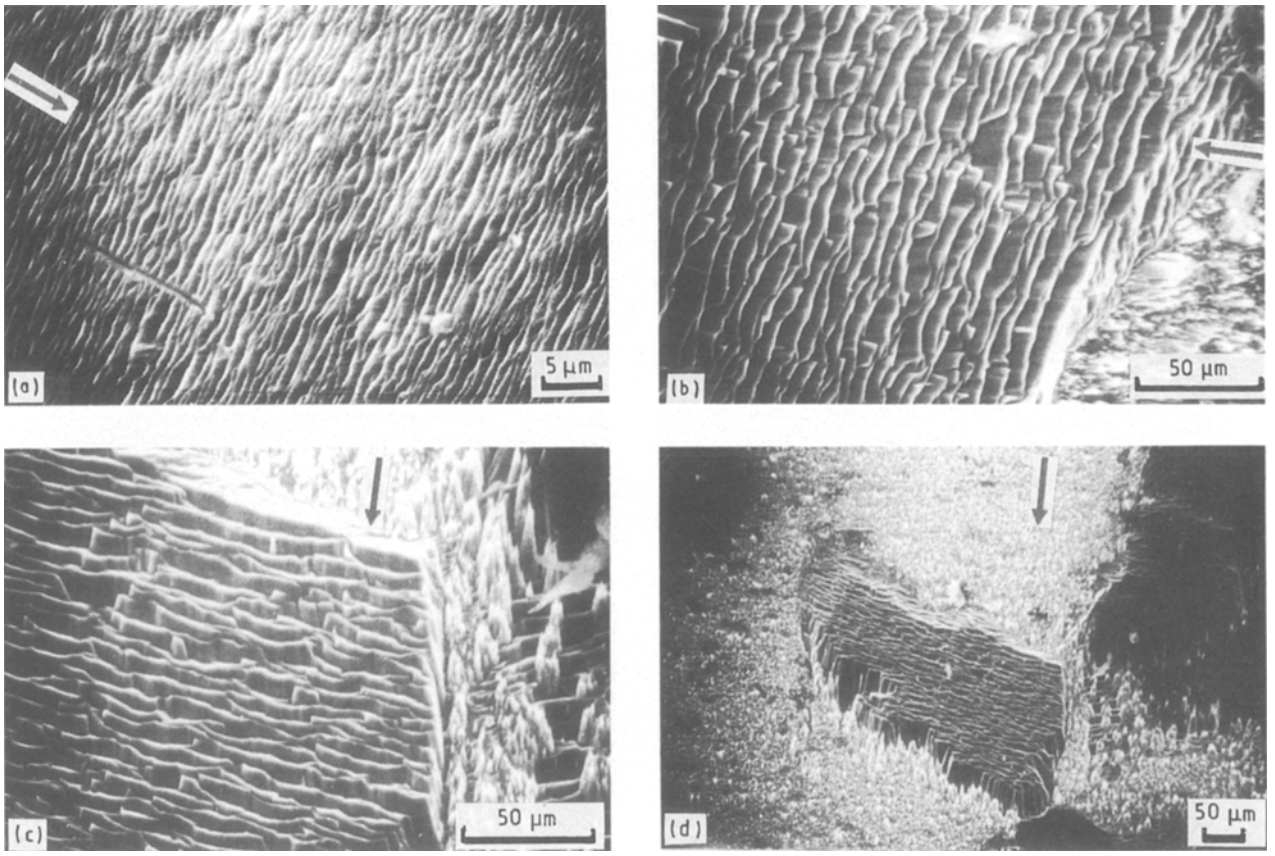

Figure 9 Electron micrographs showing corrugated terrace steps. (a) An unseeded surface, (b–d) seeded with tungsten. (b, c) The same corrugated structure is shown in orthogonal imaging conditions. (d) A lower magnification micrograph of (c), the low erosion of the faceted grain relative to the adjacent grains is clearly visible; dose = 9×10^{18} ions cm^{-2} in (a) and 5×10^{19} ions cm^{-2} in (b–d). The arrow indicates the direction of ion incidence.

Finally, we observed corrugated terrace steps on some grains (Fig. 9). Generally, corrugations, terraces or ripple structures are formed when surfaces are irradiated at oblique incidence [27]. The terraced structures are thought to form as a result of the overlap, extension and subsequent modification of etch pits. It can be seen from the micrographs that the plane of the terrace is oriented nearly parallel to the direction of the ion flux, while the ledge of the step is aligned approximately perpendicular to the ion-beam direction. Also, the dimensions of the facets are large at increased ion dose. Such an aligned repetitive topography is typical of semiconductor materials [28–31] that are rendered amorphous by ion bombardment. However, Carter *et al.* [27] have pointed out that ripples or terraced structures formed in metals, may not be correlated with the projected ion-beam direction, as is the case in amorphous media. Because aluminium is prone to oxide formation, the grains containing terraced structures may plausibly be in the amorphous Al_2O_3 phase. Sputtering yield measurements show that Al_2O_3 has a substantially lower yield

than for pure aluminium [32]. This is also supported from the micrograph presented in Fig. 9d showing the terraced grain eroded little compared to the neighbouring cone-covered grain.

4. Conclusions

The present target is a not-too-small-grained material, as seen from the micrographs. Therefore, the sputtering structures, of which cones are prominent, are essentially characteristic of single crystals. Although evidence indicates that aluminium cones were impurity induced, no increase in cone density was found by deliberate deposition of impurities, indicating the importance of local crystal orientation for the formation of cones. The cone apex angles can be well predicted by TFM or ZBL potentials used for low-energy ion scattering. Several characteristic features of cones were found. A few cones are tailed with ridges on the upstream sides, some have deformations such as bending or drooping. New features of cones observed are the coalescence of several neighbouring cones and the splitting of the cone tip. It seems that the redeposition of sputtered atoms and the preferential condensation of seed atoms play some role in their formation. The surface topography of a few grains is decorated with corrugated repetitive structures similar to those found in amorphous semiconductors, suggesting the grains involved to be in the amorphous Al_2O_3 phase.

Acknowledgements

The authors thank RSIC, Bose Institute, Calcutta for the SEM work, and I. Das, TIFR, Bombay, for performing the EDX analysis.

References

1. G. CARTER, B. NAVINŠEK and J. L. WHITTON, in "Sputtering by Particle Bombardment II", edited by R. Behrisch (Springer, Berlin, Heidelberg, 1983) p. 231.
2. O. AUCIELLO, in "Ion Bombardment Modification of Surfaces: Fundamentals and Applications", edited by O. Auciello and R. Kelly (Elsevier, Amsterdam, 1984) p. 435.
3. D. GHOSE and S. B. KARMOHAPATRO, *Adv. Electron. Electron Phys.* **79** (1990) 73.
4. H. H. ANDERSEN and H. L. BAY, in "Sputtering by Particle Bombardment I", edited by R. Behrisch (Springer, Berlin, Heidelberg, 1981) p. 145.
5. R. BERNAS, Thèse de Docteur des Sciences, Université de Paris (1954).
6. G. K. WEHNER, *J. Vac. Sci. Technol.* **A 3** (1985) 1821.
7. H. R. KAUFMAN and R. S. ROBINSON, *ibid.* **16** (1979) 175.
8. R. S. ROBINSON and S. M. ROSSNAGEL, in "Ion Bombardment Modification of Surfaces: Fundamentals and Applications", edited by O. Auciello and R. Kelly (Elsevier, Amsterdam, 1984) p. 299.
9. M. TANEMURA and F. OKUYAMA, *Nucl. Instrum. Meth. B* **47** (1990) p. 126.
10. A. K. SEN and D. GHOSE, *J. Mater. Sci. Lett.* **10** (1991) 1304.
11. *Idem, Nucl. Instrum. Meth. B* **61** (1991) 253.
12. J. LINDHARD, *Mat. Fys. Medd. Dan. Vid. Selsk.* **34** (1965) No. 14.
13. M. J. WITCOMB, *J. Mater. Sci.* **9** (1974) 1227.
14. D. GHOSE, *Jpn J. Appl. Phys.* **18** (1979) 1847.
15. G. MOLIÈRE, *Z. Naturforsch.* **2a** (1947) 133.
16. J. F. ZIEGLER, J. P. BIERSACK and U. LITTMARK, in "The Stopping and Range of Ions in Solids", Vol. 1, edited by J. F. Ziegler (Pergamon, New York, 1985).
17. TH. FAUSTER, *Vacuum* **38** (1988) 129.
18. G. W. LEWIS, G. CARTER, M. J. NOBES and S. A. CRUZ, *Rad. Eff. Lett.* **58** (1981) 119.
19. O. AUCIELLO and R. KELLY, *Rad. Eff.* **66** (1982) 195.
20. S. MORISHITA, M. TANEMURA, Y. FUJIMOTO and F. OKUYAMA, *Appl. Phys. A* **46** (1988) 313.
21. G. CARTER and M. J. NOBES, in "Ion Bombardment Modification of Surfaces: Fundamentals and Applications", edited by O. Auciello and R. Kelly (Elsevier, Amsterdam, 1984) p. 163.
22. M. NINDI and D. STULIK, *Vacuum* **38** (1988) 1071.
23. S. MORISHITA and F. OKUYAMA, *J. Vac. Sci. Technol. A* **9** (1991) 331.
24. J. BELSON and I. H. WILSON, *Phil. Mag. A* **45** (1982) 1003.
25. I. H. WILSON, J. BELSON and O. AUCIELLO, in "Ion Bombardment Modification of Surfaces: Fundamentals and Applications", edited by O. Auciello and R. Kelly (Elsevier, Amsterdam, 1984) p. 225.
26. S. E. DONNELLY, *Rad. Eff.* **90** (1985) 1.
27. G. CARTER, M. J. NOBES and J. L. WHITTON, *Appl. Phys. A* **38** (1985) 77.
28. G. CARTER, G. W. LEWIS, M. J. NOBES, J. COX and W. BEGEMANN, *Vacuum* **34** (1984) 445.
29. G. CARTER, *ibid.* **34** (1984) 819.
30. S. DUNCAN, R. SMITH, D. E. SYKES and J. M. WALLS, *ibid.* **34** (1984) 145.
31. T. K. CHINI, S. R. BHATTACHARYYA, D. GHOSE and D. BASU, *Jpn J. Appl. Phys.* **30** (1991) 2895.
32. G. BETZ and G. K. WEHNER, in "Sputtering by Particle Bombardment II", edited by R. Behrisch (Springer, Berlin, Heidelberg, 1983) p. 11.

Received 30 September 1991
and accepted 30 July 1992